30th NENE 2021
September 6 - 9
BLED-SLOVENIA
International Conference Nuclear Energy for New Europe

A Neural Network Model for the Microlayer Evaporation in Wall Boiling Flows

I. Evdokimov, S. Hänsch
Helmholtz-Zentrum Dresden-Rossendorf e.V.
Bautzner Landstraße 400
01314, Dresden, Germany
i.evdokimov@hzdr.de, s.haensch@hzdr.de

ABSTRACT

In this work we present a Feed-Forward Neural Network (FFNN), which was trained by a small set of direct numerical simulation (DNS) data with the aim to predict microlayer profiles and volumes under different wall boiling conditions. Various configurations of such machine learning (ML) models were studied and introduced into the OpenFOAM open source CFD solver. The training data consists of interface-tracking simulation results of the early bubble growth stages. The computed microlayer-to-bubble volume ratio allowed the trained FFNN model to be embedded into the Rensselaer Polytechnic Institute (RPI) wall boiling model of OpenFOAM, which was extended in order to account for an additional microlayer evaporation term. Whilst the overall evaporation component remains unchanged in magnitude, the proposed model does distinguish between the evaporation contributions from the upper curved bubble surface and from the microlayer region. The FFNN extended RPI wall boiling model is applied to an experimental case for water under atmospheric pressure, for which the microlayer evaporation is expected to be significant. The FFNN extended RPI wall boiling model is shown to predict reasonable contributions of the different evaporation mechanisms.

1 INTRODUCTION

Nucleate boiling is one of the most challenging fields of research in multiphase flows. The understanding of the tightly coupled mass, momentum and energy transfers is complicated by the wide range of physical length scales involved. The vapour generation during nucleate boiling at atmospheric pressure is known to occur not only from the upper surface of the bubble, but also from the so-called microlayer, a thin layer of liquid forming between the wall and the underside of the bubble growing at a heated wall. Recent experimental (e.g. [3]) as well as computational studies (e.g. [4], [5]) have demonstrated that the microlayer configuration and contribution to bubble growth depends on the particular conditions. Amongst other factors the microlayer thickness is seen to depend on the working fluid used and the wall superheat applied. First attempts have been made to include representations of microlayer evaporation into wall boiling CFD on the component-scale [6]. However, the models used for this are semi-empirical and based on the limited microlayer data available so far. The extremely small length and time scales involved in microlayer formation and evaporation make microscopic experiments and simulations very challenging. This paper presents an alternative approach of developing microlayer evaporation models using a small set of DNS data on microlayer formation for different wall superheats. The DNS data were fed to a neural network, which provides a ML model predicting the microlayer volumes under different boiling conditions.

2 THE DNS DATA SET

The DNS simulations were performed with PHASTA (”Parallel Hierarchic Adaptive Stabilized Transient Analysis”), a three-dimensional finite-element based code with both interface-tracking [7] and phase-change capabilities [8].

The applied fluid properties for our studies are the ones for steam and water at atmospheric pressure conditions. The fully three-dimensional computational domain used was made of a 1x1x1mm cube with outflow boundary conditions on the top and at the sides, and a no-slip condition at the bottom wall. The domain was initialised at three different superheat levels of 5, 10 and 15K. A tiny vapour seed of only 80 microns is initialised in the centre of the domain. This bubble seed grows radially outwards via applying the phase change model. The focus of the computations lies on the region near the wall, where the microlayer is forming underneath the bubble, and the mesh was refined considerably there to allow its resolution.

Results of different stages of the bubble growth at the different superheat levels are illustrated in Figure 1. Qualitative results of earlier two-dimensional CFD studies with other interface-tracking codes (e.g. [4]) could be reproduced in 3D for the first time. The results presented here show the formation of hemispherical bubbles at higher growth rates with extensive microlayers being formed. The microlayer thickness is seen to increase with the bubble growth rate.

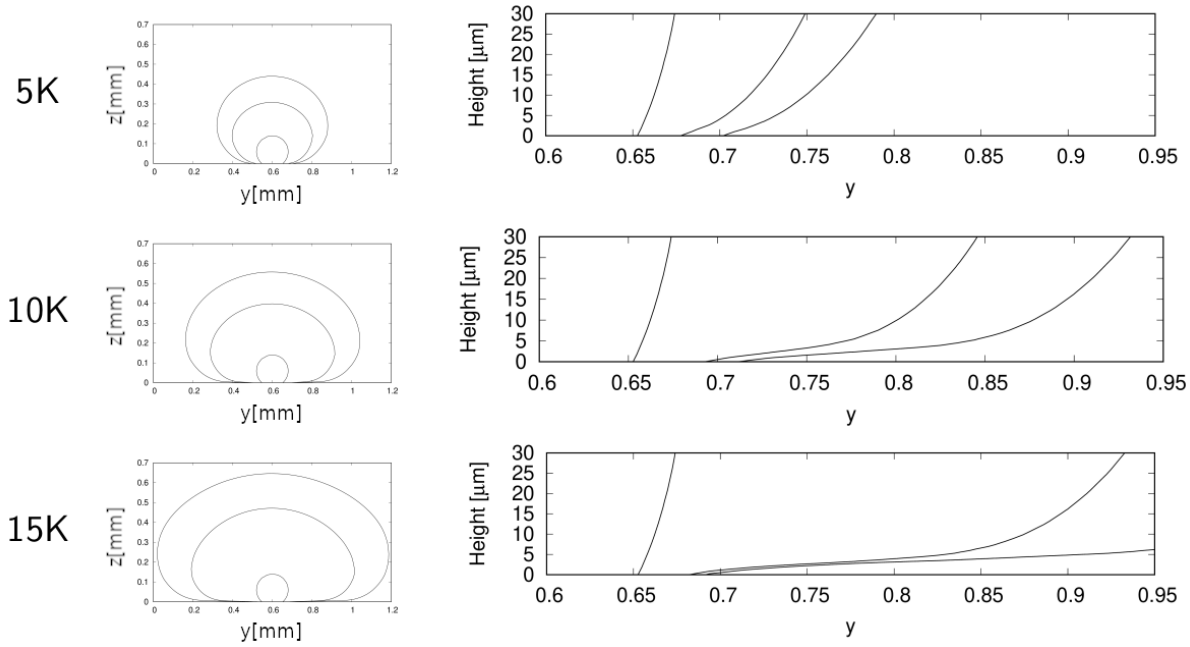

Figure 1: Computed bubble shapes (left) and enlarged region near nucleation site which outlines microlayer near the wall (right) at different times for the various wall superheats of 5, 10 and 15K investigated. ”Height” refers to wall distance and microlayer thickness.

3 DATA MINING & MACHINE LEARNING MODEL

The designed ML model uses only three main parameters as an input and predicts the microlayer volume according to equation:

$$V_{ml} = f(R, \Delta T_{sup}, V_{bub}), \tag{1}$$

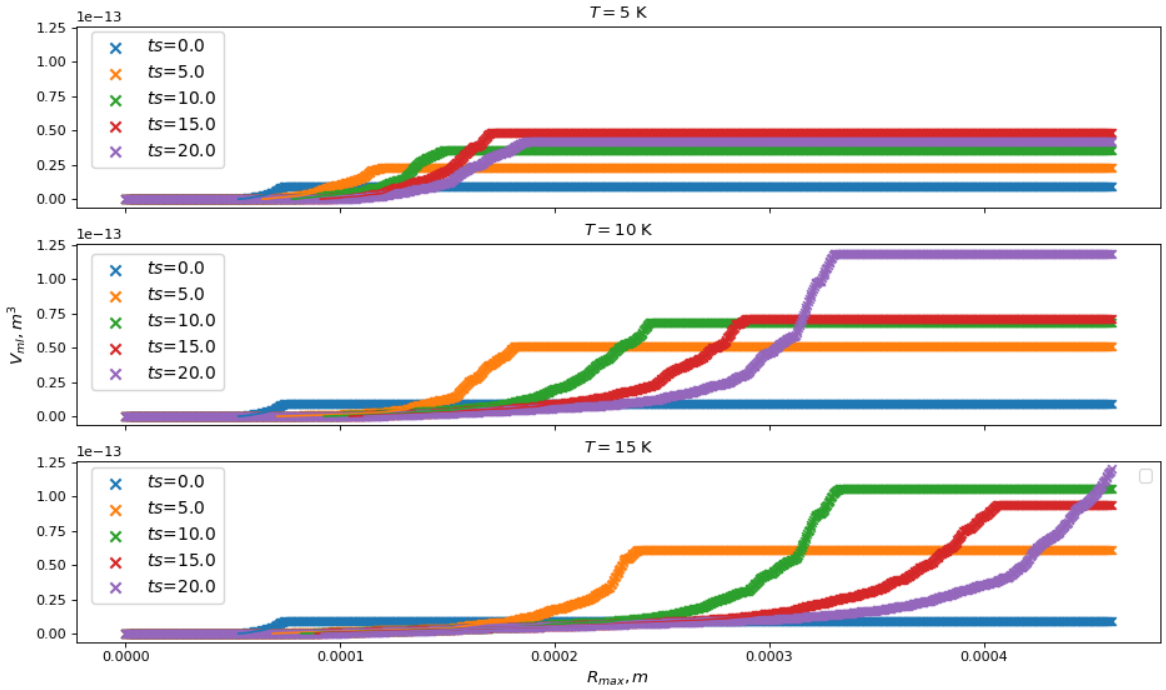

Figure 2: Raw data scatterplot for non-normalized values. Colors represent different subsets $V_{bub} = const$ of the whole dataset corresponding to different timesteps for which DNS solutions are obtained

where

V_{ml} – microlayer volume equal to total fluid volume under bubble surface (Figure 1, right) up to maximum radius R, ΔT_{sup} – superheat temperature, R – radius defining microlayer boundary, V_{bub} – is bubble volume.

Due to RPI model design relying on so called *departure diameter* D_{dep}, we conveniently assume $R = 0.5 \cdot D_{dep}$ and $V_{bub} = f(D_{dep})$ in OpenFOAM solver. RPI implements separate model for calculation of D_{dep} which is out of scope of present work.

The input data for the training process were obtained from the high-resolution bubble contours in Figure 1 in the form of a table. As Eq. (1) suggests the physical time is excluded from the data and the microlayer evolution is defined via the bubble volume growth V_{bub}. It stems from technical requirements of the top-level RPI model which operates with aggregate quantities and makes inference with smaller timescales practically infeasible.

The radius R defines an upper limit of the volume integral for obtaining V_{ml} from the training data. It is reserved in case we want to change the criteria for the upper microlayer integration limit, i.e. if the top-level model utilising the ML inference sets the microlayer boundary at e.g. $\frac{2}{3}D_{dep}$ or $\frac{1}{3}D_{dep}$ or will use more complex definition with contact angle. It is expected that such effects should have minor influence and we assume their contribution can not be tracked with aggregate models.

The raw data were normalised to global maximums and normalisation coefficients are supposed to pass around along with the serialised ML model. Figure 2 illustrates raw data points and Figure 3 demonstrates normalized values including some values interpolated by FFNN, i.e. missing in original training dataset.

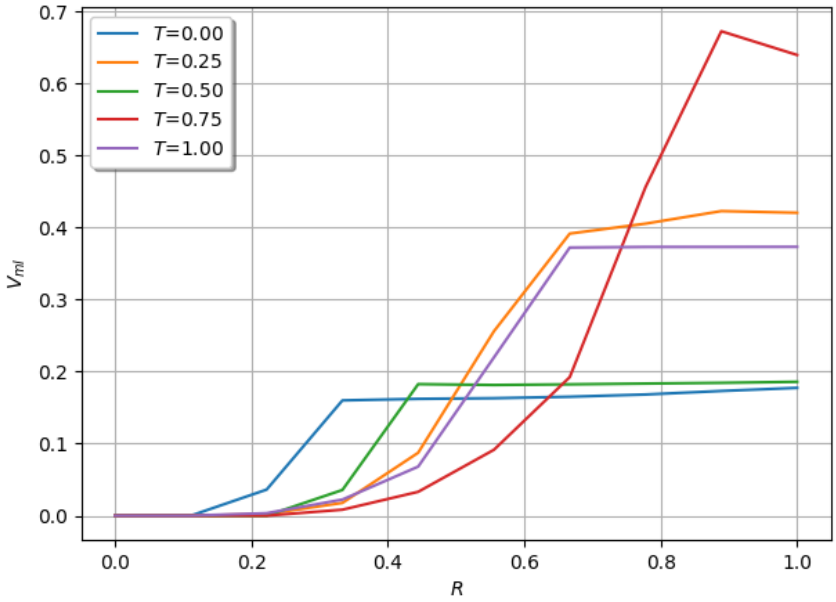

Figure 3: ML model output example. V_{ml} normalized values are predicted against normalized features values in according to eq. 1. Known dataset points are at $T = 1.0$ or $T_{sup} = 15K$ and other inferred interpolated subsets belong to $T = const$, $V_{bub} = const$. Color represents various random $V_{bub} = const$ values similar to scatter plot on the Fig. 2

4 INCLUSION OF THE ML MODEL INTO THE WALL BOILING MODEL

4.1 Extension of the RPI model with a microlayer term

This section briefly describes how the ML microlayer model is integrated into the existing wall boiling model in *HZDRmultiphaseEulerFoam* [11]. The *HZDRmultiphaseEulerFoam* solver uses the RPI wall boiling model [9] based on the assumption that the wall heat flux can be divided via

$$\dot{q}_{wall} = \dot{q}_C + \dot{q}_Q + \dot{q}_E \tag{2}$$

into the three components of a convective $\dot{q}_C$, quenching $\dot{q}_Q$ and evaporation heat flux $\dot{q}_E$.

The evaporation component should not be modified since its magnitude is governed by the departure diameter of the bubble, which does not depend on where the generated steam was produced (upper bubble surface or microlayer). However, the microlayer evaporation reduces the wall temperature underneath the bubble diminishing the contribution of the quenching component after the bubble has lifted off the wall [10].

It is proposed to reduce the quenching heat flux component by the microlayer evaporation term while keeping the default definition for all the other heat flux components. By reducing the quenching component, another on has to increase, which ideally would be the evaporative component. Increasing evaporation component leads to increased vapor generation on the wall. The updated equation for quenching heat flux:

$$\dot{q}_Q = A2 \cdot \left(h_Q(Tw - Tl) - \dot{q}_{ml} \right) \tag{3}$$

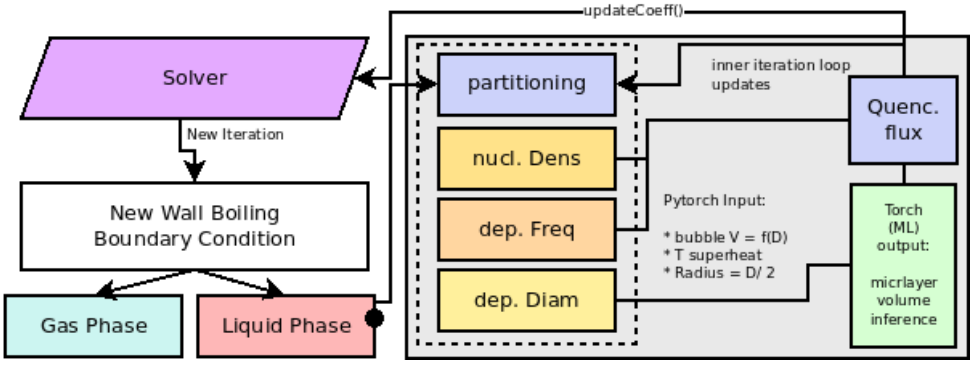

Figure 4: `mlAlphatWallBoilingWallFunction` major components and their interaction.

where

$$\dot{q}_{ml} = V_{ml} \cdot \rho_f \cdot h_{fg} \cdot f \cdot n \tag{4}$$

The term V_{ml} in Eq. (4) is an inferred microlayer volume provided by the corresponding output of the ML model from Eq. (1). Departure frequency f, nucleation density n are outputs of the corresponding standard RPI sub-models (also depicted on the Figure 4). Variables ρ_f and h_{fg} are correspondingly liquid density and evaporation heat transfer coefficient.

4.2 OpenFOAM deployment

The ML model is deployed via injection of the V_{ml} (Eq. (4)) inference logic into OpenFOAM standard `alphatWallBoilingWallFunction` boundary condition. The ML-enabled `alphat.liquid` boundary condition is similar to the original boundary condition with exempt of the `pyTorch` model specification `torchModel "NN_Water_Lean.pt"` and normalisation coefficient input fields. Figure 4 illustrates the various components of the modified `mlAlphatWallBoilingWallFunction` class.

The boundary condition code calculates the RPI submodels for the *Gas Phase* and the *Liquid Phase* when the solver calls the `updateCoeff()` function. During each boundary condition inner iteration step Torch API receives an updated wall superheat temperature and bubble departure size, and returns the inferred microlayer volume for each boundary face individually. The new boundary condition allows the microlayer volume to be computed in dependence of the departure diameter and the superheat temperature, which is believed to have a significant effect on the microlayer thickness as demonstrated by several works ([4], [5]). The departure diameter allows inferred microlayer volume to be dynamic in response to changing model conditions and helps to establish a connection with RPI model, it may be replaced with physical time as long as top-level simulation model allows that.

5 TEST CASE

The experimental case of Lee et al. [2] measured gas void fraction and velocity profiles in a concentric annulus with a heated inner tube. Working fluid is water at atmospheric pressure conditions. Under these conditions the formation of microlayers and their significant contribution to bubble growth are to be expected [4]. Various heat flux, mass flux and inlet subcooling conditions are available from the experiment. The parameters of the selected cases studied here are listed in Table 1.

Table 1: Experimental conditions of the Lee cases investigated.

Case	p	$\dot{m}[kg/m^2s]$	$\dot{q}_W[kW/m^2]$	subcooling [K]
1	atm	718.2	232.6	21.2
2	atm	718.8	320.4	21.3

A grid was chosen (20cells x 400cells) as to guarantee y+ values > 30, which is the lower limit to use wall functions with `kOmegaSST` turbulence model. The parameters for the RPI submodels are listed in Table 2. The nucleation site density N_{Ref} parameter value $5.0e5$ is different to the OpenFOAM default $9.922e5$.

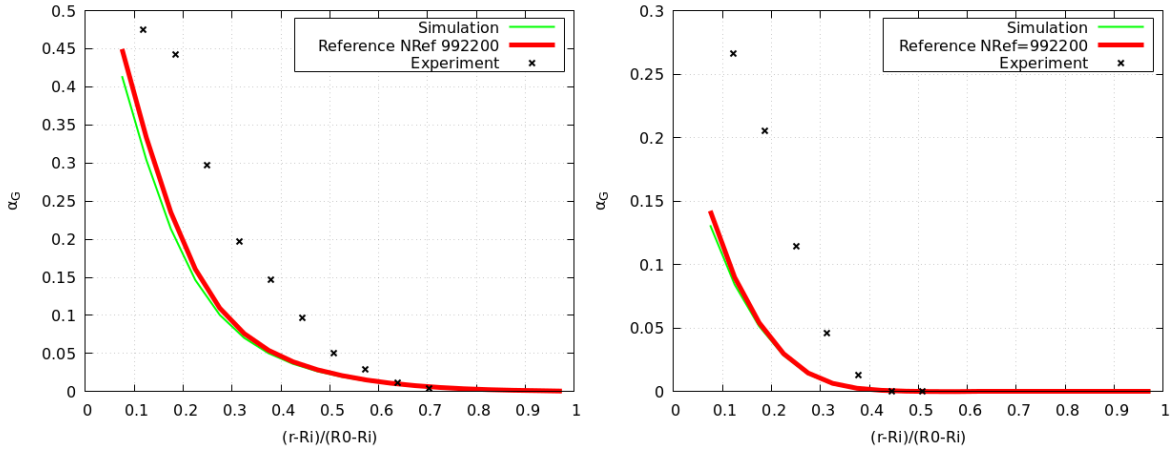

a *b*

Figure 5: Simulation results (gas/vapor phase fraction α_G) for standard RPI with $N_{Ref} = 5.0e5$ against reference default value $N_{Ref} = 9.922e5$. Figure (a) corresponds to Case 1 (a) and (b) to Case 2 Table 1. On horizontal axis, $(r - Ri)/(R0 - Ri)$ represents normalized distance between inner hot (Ri) and outer cold wall $R0$.

N_{Ref} is one of calibration constants of RPI model and provides value for nucleation site density equation in relevant sub-model. For the sake of simplicity it was decided to adjust its value while keeping standard sub-model. Lowering N_{Ref} allows to increase the wall superheat temperature and pushes ML model into a temperature interval relevant for the microlayer formation and evaporation phenomena. Compared to experimental values the reference case with $N_{Ref} = 5.0e5$ does not demonstrate any significant differences to the one with the default $N_{Ref} = 9.922e5$ (Figure 5).

Table 2: OpenFoam RPI parameters for the Lee case.

Model	Parameter	Value
N [13]	Cn	1
	N_{Ref}	5e05
	ΔT_{Ref}	45 (OF default)
d_{Dep} [14]	d_{ref}	0.002
	d_{max}	0.005
	d_{min}	1e-06
f [15]	-	-

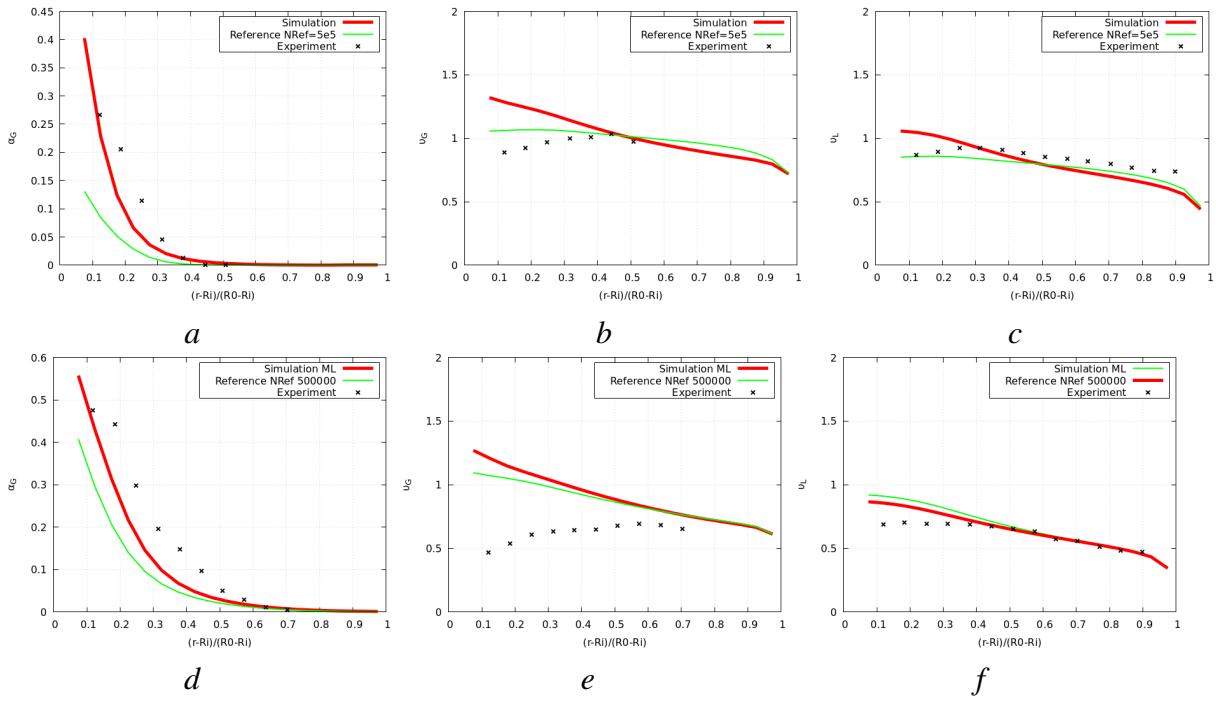

Figure 6: Simulation results, *a-c* Case 1, *d-f* Case 2 from Table 1. Plots *a, d* depict vapour fraction; *b, e* gas velocity and *c, f* liquid velocity. "Reference" label represents the OpenFOAM case with standard RPI and no microlayer contribution, Red "Simulation" results depict our results with the NN extended RPI wall boiling model accounting for microlayer evaporation.

As expected we can see a significant effect of the microlayer term upon the results for this steam-water case in Figure 6. Reducing the quenching heat flux component increases the evaporation heat flux and produces significantly larger amounts of steam. Results including the microlayer term fit better to the experimental data in case of gas/vapor phase fraction prediction and do not demonstrate significant improvements for velocity fields. The reason for minor discrepancies in velocity fields might be due to `slip` boundary conditions on hot wall.

6 CONCLUSIONS

In this paper we used a small DNS data set of the microlayer formation for the training of a neural network model that is able to predict microlayer volumes under various wall boiling conditions. The standard RPI wall boiling model in OpenFOAM was extended by a corresponding microlayer evaporation term using the ML inferred microlayer volume provided by Torch C++ API.

The NN extended RPI wall boiling model was applied to a test case. In the experimental case of [2] with water under atmospheric pressure and high wall superheats the ML model predicts significant changes in the heat flux distribution with more vapour being generated, which agrees better to the measured data.

The application of ML techniques, where experimental and computational limits hinder sufficient data collection, seems a promising alternative to the conventional development of Euler-Euler models. An interesting area for future work is the addition of available experimental data of microlayer profiles to the NN training process for more refined results and a greater variety of boiling conditions.

REFERENCES

[1] J. Garnier, E. Manon, G. Cubizolles, "Local measurments on flow boiling of refrigerant R12 in a vertical tube", Multiphase Science and Technology, 13, 2001, pp. 1–111.

[2] T.H. Lee, G.C. Park, D.J. Lee, "Local flow characteristics of subcooled boiling flow of water in a vertical concentric annulus", Int. J. Multiphas. Flow, 28, 2002, pp. 1351–1368.

[3] Y. Utaka, Y. Kashiwabara, M. Ozaki, "Microlayer structure in nucleate boiling of water and ethanol at atmospheric pressure", Int. J. Heat Mass Tran., 57, pp. 222–230, 2013.

[4] S. Hänsch, S. Walker, "The hydrodynamics of microlayer formation beneath vapour bubbles", Int. J. Heat Mass Tran., 102, 2016, pp. 1282–1292.

[5] A. Guion, S. Afkhami, S. Zaleski, J. Buongiorno, "Simulations of microlayer formation in nucleate boiling", Int. J. Heat Mass Tran., 127, pp. 1271–1284, 2018.

[6] L. Gilman, E. Baglietto, "A self-consistent, physics-based boiling heat transfer modeling framework for use in computational fluid dynamics", Int. J. Multiphas Flow, 95, pp. 35–53, 2017.

[7] S. Nagrath, K. Jansen, R.T. Lahey Jr, I. Akhatov, "Hydrodynamic simulation of air bubble implosion using a level set approach", J. Comput. Phys., 215(1), pp. 98– 132, 2006.

[8] M. Li, I. Bolotnov, "The evaporation and condensation model with interface tracking", Int. J. Heat Mass Tran., 150, pp. 119256.

[9] N. Kurul, M. Podowski, "Multidimensional effects in forced convection sub-cooled boiling", Proc. Ninth International Heat Transfer Conference, Vol. 2, pp. 21–26, 1990.

[10] S. Hänsch, S. Walker, "Microlayer formation and depletion beneath growing steam bubbles", Int. J. Multiphas Flow, 111, pp. 241–263, 2019.

[11] F. Schlegel, M. Draw, I. Evdokimov, S. Hänsch, H. Khan, R. Lehnigk, R. Meller, G. Petelin, M. Tekavčič, "HZDR Multiphase Addon for OpenFOAM", `https://rodare.hzdr.de/record/768`, 2021.

[12] J. Peltola, W. Bainbridge, R. Lehnigk, F. Schlegel, "On development and validation of subcooled nucleate boiling models for OpenFOAM Foundation Release", Proc. NURETH-18, Portland, OR, August 18–22, 2019.

[13] M. Lemmert, J. M. Chawla, "Influence of flow velocity on surface boiling heat transfer coefficient". In: Heat Transfer and Boiling, Academic Press, 1977, pp. 237–247.

[14] G. Kocamustafaogullari, M. Ishii, "Foundation of the Interfacial area transport equations and itsclosure relations", Int. J. Heat Mass Tran., 1995.

[15] G. Kocamustafaogullari, M. Ishii, "Interfacial area and nucleation site density in boiling systems", Int. J. Heat Mass Tran., 1983.